A Massively Parallel Electrochemical Approach to the Miniaturization of Organic Micro- and Nanostructures on Surfaces

Yi Zhang,† Khalid Salaita,† Jung-Hyurk Lim, Ki-Bum Lee, and Chad A. Mirkin*

Department of Chemistry and Institute for Nanotechnology, Northwestern University, Evanston, Illinois 60208

Received October 23, 2003

This paper describes a simple and convenient strategy for reducing the dimensions of organic micro- and nanostructures on metal surfaces. By varying electrochemical desorption conditions, features patterned by dip-pen nanolithography or micro contact printing and made of linear alkanethiols or selenols can be gradually desorbed in a controlled fashion. The process is referred to as electrochemical whittling because the adsorbate desorption is initiated at the exterior of the feature and moves inward as a function of time. The whittling process and adsorbate desorption were studied as a function of substrate morphology, adsorbate head and tail groups, and electrolyte solvent and salt. Importantly, one can independently address different nanostructures made of different adsorbates and effect their miniaturization based upon a judicious selection of adsorbate, applied potential, and supporting electrolyte. Some of the physical and chemical origins of these observations have been elucidated.

Introduction

There are now a variety of methods for printing and constructing organic structures on surfaces, and these methods are leading to significant advances in the understanding of the chemical consequences of miniaturization and the application of patterned surfaces in fields ranging from microbiology to electronics to catalysis. Micro contact printing (μCP)[1] and variants of it are very popular and useful approaches for printing organic structures on surfaces because they are massively parallel and allow one to control feature size typically down to 200 nm.[2] Among the scanning probe based methods,[3] Dip-pen nanolithography (DPN)[4] has emerged as a powerful tool to do highly customized work in direct-write fashion with a resolution that rivals electron beam lithography. Indeed, small organic molecules,[4a−c] oligonucleotides,[4d] proteins,[4e,f] conducting polymers,[4g,h] and sol gels[4i] all have been patterned on inorganic substrates such as Au, Ag, and SiOx with sub-50 nm resolution. Although advances have recently extended single-pen DPN approaches to parallel multipen approaches,[4j] the throughput of DPN, in the short term, cannot rival printing processes. Ideally, one would like a high throughput printing process with the resolution, alignment registration, and multi-ink capabilities of DPN.

One approach to fabricating highly miniaturized organic nanostructures is to develop procedures that controllably reduce the size of an existing organic structure. Recently, we communicated an approach to miniaturization using the concept of "electrochemical whittling",[5] Scheme 1. The idea was that if a nano- or microscale feature was made of a densely packed adsorbate on a surface, the exterior adsorbate sites would be less stable than the interior ones and prone to desorption at a lower potential. Therefore, by applying a potential in a controlled manner, one, in principle, can selectively shrink features comprised of densely packed monolayer structures.

The whittling process was inspired by several observations involving bulk self-assembled monolayers (SAMs) and nanostructured materials. First, electrochemical methods have been used to effect the bulk desorption of adsorbates from SAM-coated gold electrodes,[6] and it has been proposed that the desorption process is initiated from defect sites within a monolayer.[7] With a nano- or microfeature made of a SAM on gold, the edge sites of the feature can be viewed as being defect rich. Second, it is well-known

* Corresponding author. Email: camirkin@chem.northwestern.edu.

† These authors contributed equally to this work.

(1) (a) Kumar, A.; Whitesides, G. M. *Science* **1994**, *263*, 60. (b) Jackman, R. J.; Wilbur, J. L.; Whitesides, G. M. *Science* **1995**, *269*, 664. (c) Xia, Y.; Whitesides, G. M. *Angew. Chem., Int. Ed.* **1998**, *37*, 550. (d) Xia, Y.; Venkateswaran, N.; Qin, D.; Tien, J.; Whitesides, G. M. *Langmuir* **1998**, *14*, 363.

(2) (a) Odom, T. W.; Love, J. C.; Wolfe, D. B.; Paul, K. E.; Whitesides, G. M. *Langmuir* **2002**, *18*, 5314. (b) Cherniavskaya, O.; Adzic, A.; Knutson, C.; Gross, B. J.; Zang, L.; Liu, R. Adams, D. M. *Langmuir* **2002**, *18*, 7029.

(3) (a) Xu, S. and Liu, G. Y. *Langmuir* **1997**, *13*, 3(2), 127. (b) Amro, N. A.; Xu, S.; Liu, G. Y. *Langmuir* **2000**, *16*, 3006. (c) Zhao, J.; Uosaki, K. *Nano Lett.* **2002**, *2*, 137. (d) Schoer, J. K.; Zamborini, F. P.; Crooks, R. M. *J. Phys. Chem.* **1996**, *100*, 11086. (e) Gorman, C. B.; Carroll, R. L.; He, Y.; Tian, F.; Fuierer, R. *Langmuir* **2000**, *16*, 6312. (f) Kim, Y. T.; Bard, A. J. *Langmuir* **1992**, *8*, 1096. (g) Schoer, J. K.; Crooks, R. M. *Langmuir* **1997**, *13*, 2323. (h) Chen, J.; Reed, M. A.; Asplund, C. L.; Cassell, A. M.; Myrick, M. L.; Rawlett, A. M.; Tour, J. M.; Van Patten, P. G. *Appl. Phys. Lett.* **1999**, *75*, 624. (i) Mizutani, W.; Ishida, T.; Tokumoto, H. *Langmuir* **1998**, *14*, 7197.

(4) (a) Piner, R.; Zhu, J.; Xu, F.; Hong, S.; Mirkin, C. A. *Science* **1999**, *283*, 661. (b) Hong, S.; Mirkin, C. A. *Science* **2000**, *288*, 1808. (c) Hong, S.; Zhu, J.; Mirkin, C. A. *Science* **1999**, *286*, 523. (d) Demers, L. M.; Ginger, D. S.; Park, S.-J.; Li, Z.; Chung, S.-W.; Mirkin, C. A. *Science* **2002**, *296*, 1836. (e) Lee, K. B.; Park, S.-J.; Mirkin, C. A.; Smith, J. C.; Mrksich, M. *Science* **2002**, *295*, 1702. (f) Lee, K. B.; Lim, J. H.; Mirkin, C. A. *J. Am. Chem. Soc.* **2003**, *125*, 5588. (g) Lim, J.-H.; Mirkin, C. A. *Adv. Mater.* **2002**, *14*, 1474. (h) Maynor, B. W.; Filocano, S. F.; Grinstaff, M. W.; Liu, J. *J. Am. Chem. Soc.* **2002,** *124*, 522. (i) Su, M.; Liu, X. G.; Li, S. Y.; Dravid, V. P.; Mirkin, C. A. *J. Am. Chem. Soc.* **2002**, *124*, 1568. (j) Zhang, M.; Bullen, D.; Chung, S.-W.; Hong, S.; Kee, R. S.; Fan, Z.; Mirkin, C. A.; Liu, C. *Nanotechnology* **2002**, *13*, 212.

(5) Zhang, Y.; Salaita, K.; Lim, J. H.; Mirkin, C. A. *Nano Lett.* **2002**, *2(12)*, 1389.

(6) (a) Widrig, C. A.; Chung, C.; Porter, M. D. *J. Electroanal. Chem.* **1991**, *310*, 335. (b) Walczak, M. M.; Popenoe, D. D.; Deinhammer, R. S.; Lamp, B. D.; Chung, C.; Porter, M. D. *Langmuir* **1991**, *7*, 2687. (c) Weisshaar, D. E.; Lamp, B. D.; Porter, M. D. *J. Am. Chem. Soc.* **1992**, *114*, 5860. (d) Schneider, T. W.; Buttry, D. A. *J. Am. Chem. Soc.* **1993**, *115*, 12391. (e) Walczak, M. M.; Alves, C. A.; Lamp, B. D.; Porter, M. D. *J. Electroanal. Chem.* **1995**, *396*, 103. (f) Zhong, C.-J.; Porter, M. D. *J. Am. Chem. Soc.* **1994**, *116*, 11616. (g) Zhong, C.-J.; Zak, J.; Porter, M. D. *J. Electroanal. Chem.* **1997**, *421*, 9. (h) Yang, D.-F.; Wilde, C. P.; Morin, M. *Langmuir* **1996**, *12*, 6570.

10.1021/la030392y CCC: $27.50 © 2004 American Chemical Society
Published on Web 01/07/2004

Scheme 1

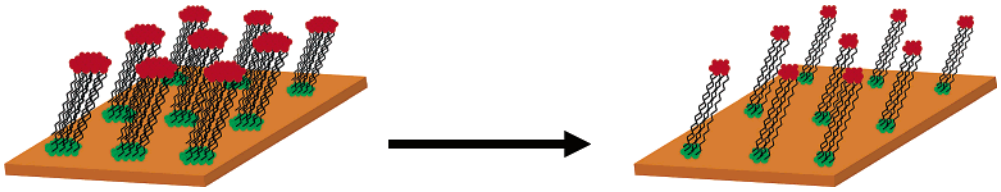

that for materials in general, surface sites are typically more reactive than bulk sites.[8] Therefore, we hypothesized that they should desorb more readily than interior sites.

In this paper, we systematically study the electrochemical whittling process and identify some of the fundamental parameters that lead to uniform and controllable miniaturization rates. The technique has been studied as a function of adsorbate headgroup, adsorbate tail group, solvent, electrolyte, and substrate morphology. Finally, we show that it can be used to miniaturize DPN generated structures as well as ones made by the parallel μCP procedure.

Experimental Section

Chemicals and Substrates. Polycrystalline Au films and Au(111) surfaces were prepared by literature procedures.[9] 16-Mercaptohexadecanoic acid (MHA) (90%), 1-octadecanethiol (ODT) (98%), KOH (semiconductor-grade purity), $LiOH{\cdot}H_2O$ (99.995%), NaOH (99.99%), ferrocene (98%), $(CH_3CH_2)_4NBF_4$ (99%), and $[CH_3(CH_2)_3]_4NBF_4$ (99%) were purchased from Aldrich Chemical Co. Ethanol (ACS/USP grade) was purchased from Pharmcoproducts Inc. Acetonitrile (reagent grade) and methylene chloride (99.9%) were purchased from Fisher Scientific. All chemicals were used as received. Dioctadecane diselenide (DODDSe) was synthesized and purified according to literature procedures.[10]

Dip-Pen Nanolithography, Micro Contact Printing, and Atomic Force Microscopy Imaging. DPN of organic nanostructures was performed with an atomic force microscope (AFM, CP, Veeco/ThermoMicroscopes, Sunnyvale, CA) equipped with a 100-μm scanner with closed-loop scan control and commercial lithography software (DPNWrite, DPN System-1, NanoInk Inc., Chicago, IL). Gold-coated Si_3N_4 AFM cantilevers (Microlever, Veeco/ThermoMicroscopes, Sunnyvale, CA) with a spring constant of 0.05 N/m were used for patterning. MHA-coated tips were prepared by immersing the cantilevers in an acetonitrile solution saturated with MHA for a few seconds, followed by blow drying with compressed difluoroethane (Dust-off, Ted Pella Inc., Redding, CA). ODT-coated tips were prepared by thermal evaporation of ODT onto the tips at 65 °C for 30 min. DODDSe-coated tips were also prepared by thermal evaporation of DODDSe onto the tips at 150 °C for 1 h in an evacuated flask. All DPN patterning experiments were carried out under ambient laboratory conditions (~30% relative humidity, ~20 °C) and as previously reported.[4a−4c] Subsequent imaging of the DPN-generated patterns and the electrochemically whittled patterns was done using a clean AFM tip under conditions identical to those used for patterning. All images are in lateral force mode[4] except where noted otherwise.

MHA and ODT micropatterns were generated via μCP.[1] Stamps were fabricated by placing a photolithographically prepared master (by using photomask from ADTEK, Quebec, Canada) in a glass Petra dish, followed by pouring over the master a mixture of polydimethlysiloxane (PDMS, Sylgard 184, Dow Corning, Midland, MI) in the ratio of 10:1 (v:v) monomer to initiator. After 1 h of degassing, the elastomer was cured for 2 h at 60 °C and then gently peeled from the master. The stamp was "inked" with a 10 mM ethanol solution of ODT or MHA and dried under N_2 flow. Organic microstructures were generated by bringing the stamp (by hand) into contact with a clean Au substrate for about 3 s.

Electrochemical Desorption. To effect electrochemical whittling, the substrate (polycrystalline Au films and Au(111) surfaces) with prepatterned organic monolayer features was placed into the electrochemical cell and used as the working electrode in a three-electrode configuration (Bioanalytical System potentiostat, BAS 100B). The counter electrode was a Pt wire, and all potentials were recorded with respect to an Ag/AgCl reference electrode. The electrochemical whittling was performed by applying a reductive potential to the substrate for a designated period of time. The cyclic voltammograms for the reductive desorption of MHA, ODT, and DODDSe SAMs were also carried out using the same setup. Aqueous solutions of KOH, LiOH, and NaOH (0.5 M), respectively, were used as the supporting electrolyte and were degassed with N_2 before use. Following electrochemical desorption, the substrates were rinsed with Nanopure water and ethanol, respectively, and then dried with N_2 gas. The patterned areas of the surfaces were imaged subsequently by AFM, by making use of alignment marks,[4c] to measure the change in feature size of the organic structures. For the electrochemical whittling of MHA nanostructures in methylene chloride (containing 0.1 M $(CH_3CH_2)_4NBF_4$ or 0.1 M $[CH_3(CH_2)_3]_4NBF_4$), a polished silver fiber was used as a reference electrode and referenced to ferrocene.

Results and Discussion

Electrochemical Whittling of MHA Nanostructures at Different Potentials. By use of a negative potential to a patterned gold electrode, the feature size of MHA nanostructures can be gradually but significantly reduced. During this reductive desorption process, the periphery of the MHA nanostructures on the electrode surface is presumed to undergo the following reaction: $R{-}S{-}Au + e^- \rightarrow R{-}S^- + Au$, based on literature precedent.[6a] Since reductive desorption is strongly dependent on the applied potential,[6] it is useful to study the whittling process under different potentials.

Electrode potential dramatically affects the whittling rate of MHA nanostructures, Figure 1. The onset of whittling is at −750 mV vs Ag/AgCl in aqueous solution with 0.5 M MOH (M = K, Na, or Li) as the supporting electrolyte. Electrode potentials more positive of this value (e.g., −700 mV) do not effect a decrease in feature size even when the electrode is held at such potentials for extended periods of time (2 min), Figure 1A,B. In the case of KOH as the supporting electrolyte, when a potential of −750 mV is applied to a substrate with a series of different diameter MHA dot features, the features decrease in diameter at a rate of approximately 50 nm/min, regardless of initial feature size (range studied 500−80 nm), Figure 1C,D. In general, more negative potentials accelerate feature size reduction. For example, at electrode potentials of −800, −850, and −900 mV, the whittling rate increases to ~2 nm/s (Figure 1E,F), 9 nm/s (Figure 1G,H), and 50 nm/s (Figure 1I,J), respectively. The uniformity of the

(7) (a) Yang, D.-F.; Morin, M. *J. Electroanal. Chem.* **1997**, *429*, 1. (b) Yang, D.-F.; Morin, M. *J. Electroanal. Chem.* **1998**, *441*, 173. (c) Poelman, M. and Buess-Herman, C. *Langmuir* **1999**, *15*, 2194. (d) Mulder, W. H.; Calvente, J. J.; Andreu, R. *Langmuir* **2001**, *17*, 3273. (e) Wano, H.; Uosaki, K. *Langmuir* **2001**, *17*, 8224. (f) Hobara, D.; Miyake, K.; Imabayashi, S.; Niki, K.; Kakiuchi, T. *Langmuir* **1998**, *14*, 3590.

(8) McCash, E. M. *Surface chemistry*; Oxford University Press: New York, 2001.

(9) (a)Weinberger, D. A.; Hong, S.; Mirkin, C. A.; Wessels, B. W.; Higgins, T. B. *Adv. Mater.* **2000**, *12*, 1600. (b) Ross, C. B.; Sun, L.; Crooks, R. M. *Langmuir* **1993**, *9*, 632.

(10) Griffin, S.; Klayman, D. *J. Am. Chem. Soc.* **1973**, *95*, 197.

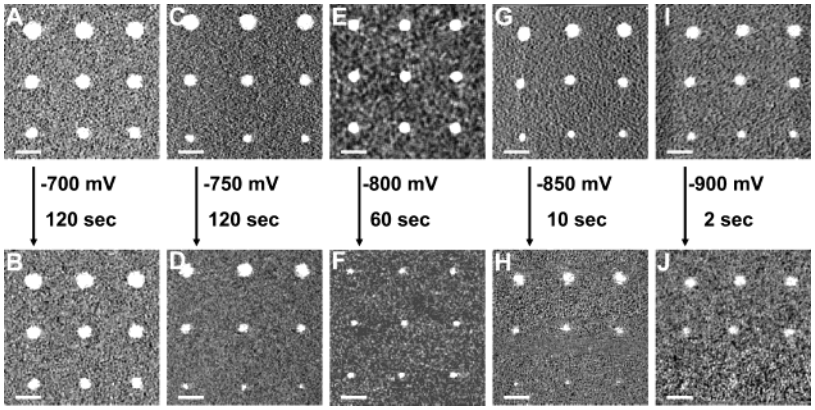

Figure 1. LFM images of DPN-generated MHA patterns before (upper) and after (below) electrochemical whittling at different potentials with different time lengths. The bar is 500 nm.

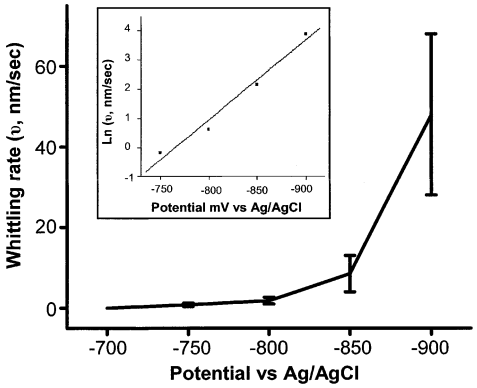

Figure 2. A plot of electrochemical whittling rate (*v*) of MHA nanostructures as a function of the desorption potential. Each data point was averaged from three independent experiments. In each experiment nine MHA dots were measured before and after whittling. The whittling times applied at each potential were 120 s (−700 mV), 120 s (−750 mV), 30 s (−800 mV), 10 s (−850 mV), and 2 s (−900 mV), respectively. Inset, exponential dependence of the average whittling rate (*v*) on the whittling potential.

resulting features is better at slower whittling rates (i.e., the ones obtained at less negative electrode potentials). Interestingly, an exponential dependence of the average whittling rate (*v*) on whittling potential was found (Figure 2). This phenomenon is consistent with a kinetic model for the reductive desorption of alkanethiol SAMs previously reported by Mulder et al.,[7d] indicating that DPN-generated MHA nanostructures behave similarly to closely packed alkanethiol domains under reductive potentials. Other studies done by our group have shown that DPN generated patterns of MHA and ODT, respectively, consist of psuedo-crystalline monolayers comparable to those obtained via bulk deposition methods.[4a]

Electrochemical Whittling of MHA Nanostructures as a Function of Electrolyte. Electrochemical whittling of MHA nanostructures also was performed in different media and studied as a function of solvent and supporting electrolyte. In all cases, whittling can be observed, but the potential at which desorption is initiated and the whittling rate are highly dependent upon the type of supporting electrolyte, Table 1. In addition, the whittling process is generally more uniform under aqueous conditions as compared with the organic media studied. This is supported by the AFM images obtained postwhittling and the standard deviation in whittling rates, Table 1.

It is interesting to note that the whittling rate in aqueous media increases with increasing cation size (LiOH < NaOH < KOH). At an electrode potential of −750 mV, the average whittling rate in 0.5 M aqueous MOH (M = K^+, Na^+, or Li^+) solution was 50 ± 25 nm/min for KOH, 16 ± 7 nm/min for NaOH, and 6 ± 3 nm/min for LiOH. In all three cases, in general more negative electrode potentials lead to more rapid but less controllable whittling rates.

The slower whittling rate in LiOH solutions relative to KOH and NaOH solution is consistent with the results reported previously by Porter et al.,[6a] who studied bulk SAMs and concluded that greater overpotentials were required for desorption of SAMs in the presence of Li^+ ions relative to $K^+$and Na^+ ions. This may be due to the fact that these ions are strongly solvated in water, especially in the case of Li^+; indeed, solvation changes the effective size of the cations making solvated Li^+ the largest followed by solvated Na^+ and then solvated K^+.[6a,11] This increase in size affects their ability to approach the Au−S site (the site of desorption) and compensate the charge generated upon reduction, which slows down the desorption or whittling rate. This type of effect is reminiscent of the ion-gated electron transfer observed in the context of a variety of redox-active SAMs.[12]

To investigate the significance of cation size in a media where solvation is not as important as in the aqueous alkali metal system above, electrochemical whittling was studied in CH_2Cl_2 as a function of cation size. Two supporting electrolytes were studied, 0.1 M $(CH_3CH_2)_4NBF_4$ or 0.1 M $[CH_3(CH_2)_3]_4NBF_4$. Results indicated that electrochemical whittling of MHA nanostructures in 0.1 M $(CH_3CH_2)_4NBF_4$ could be initiated and controllably carried out at −300 to −400 mV vs Fc/Fc^+. For example, 300 nm diameter MHA dots (Figure 3A) were reduced to ∼200 nm (Figure 3B) after applying a potential of −385 mV vs Fc/Fc^+ for 60 s. Applying a potential of −460 mV vs Fc/Fc^+ for 1 min resulted in complete removal of the MHA dots (∼450 nm) from the surface (Figure 3C,D). In contrast, when a larger cation is used in the form of 0.1 M $[CH_3(CH_2)_3]_4NBF_4$ as the supporting electrolyte, the onset of whittling is substantially more negative, −900 mV vs Fc/Fc^+ mV. As shown in panels A and B of Figure 4, 680 nm diameter MHA dots (Figure 4A) were reduced to 350 nm (Figure 4B) after applying a potential of −1270 mV vs Fc/Fc^+ for 60 s. For comparison purposes, applying a potential of −720 mV vs Fc/Fc^+ for 1 min resulted in no change of the MHA dot size (Figure 4C,D). From these

(11) Voet, D. Voet, J. G. *Biochemistry*, 2nd ed.; J. Wiley & Sons: New York, 1995; Chapter 2.

(12) (a) Campbell, D. J.; Herr, B. R.; Hulteen, J. C.; VanDuyne, R. P.; Mirkin, C. A. *J. Am. Chem. Soc.* **1996**, *118*, 10211. (b) Caldwell, W. B.; Campbell, D. J.; Chen, K. M.; Herr, B. R.; Mirkin, C. A.; Malik, A.; Durbin, M. K.; Dutta, P.; Huang, K. G. *J. Am. Chem. Soc.* **1995**, *117*, 6071. (c) Walter, D. G.; Campbell, D. J.; Mirkin, C. A. *J. Phys. Chem. B* **1999**, *103(3)*, 402

Table 1. Data for Electrochemical Whittling as a Function of Electrolyte, Surface, and Whittling Potential

adsorbate	electrolyte	surface	whittling potential (mV)	whittling rate[a] (nm/min)	onset potential (mV)
MHA	0.5 M KOH aqueous solution	polycrystalline Au	−750 (vs Ag/AgCl)	50 ± 25	−750 (vs Ag/AgCl)
MHA	0.5 M NaOH aqueous solution	polycrystalline Au	−750 (vs Ag/AgCl)	16 ± 7	−750 (vs Ag/AgCl)
MHA	0.5 M LiOH aqueous solution	polycrystalline Au	−750 (vs Ag/AgCl)	6 ± 3	−750 (vs Ag/AgCl)
MHA	0.1 M $(CH_3CH_2)_4NBF_4$ in CH_2Cl_2	polycrystalline Au	−385 (vs Fc/Fc^+)	310 ± 290	−200 (vs Fc/Fc^+)
MHA	0.1 M $[CH_3(CH_2)_3]_4NBF_4$ in CH_2Cl_2	polycrystalline Au	−1270 (vs Fc/Fc^+)	280 ± 170	−900 (vs Fc/Fc^+)
MHA	0.5 M KOH aqueous solution	Au(111)	−750 (vs Ag/AgCl)	35 ± 9	−750 (vs Ag/AgCl)
DODDSe	0.5 M KOH aqueous solution	polycrystalline Au	−450 (vs Ag/AgCl)	70 ± 36	−450 (vs Ag/AgCl)
ODT	0.5 M KOH aqueous solution	polycrystalline Au	−1000 (vs Ag/AgCl)	96 ± 37	−850 (vs Ag/AgCl)

[a] The whittling rate was averaged from three independent experiments. In each experiment the change in diameter of nine dots was measured before and after whittling. The deviation corresponds to variations in the measured diameter of all dots and persists even on dots generated on the same sample.

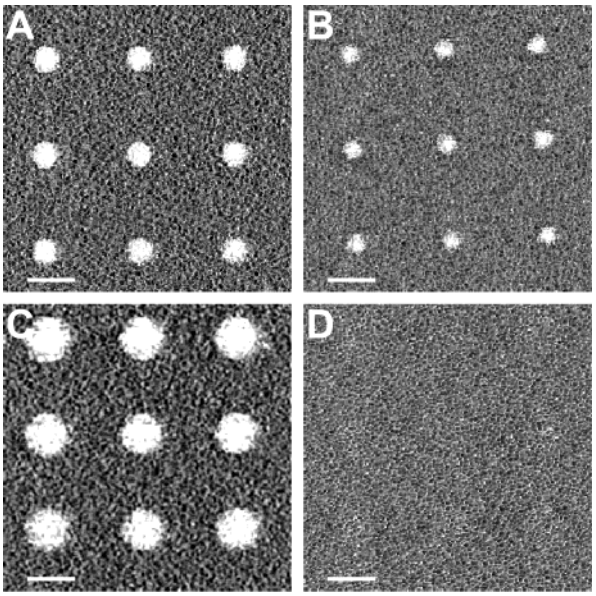

Figure 3. LFM images of DPN-generated MHA patterns before and after electrochemical whittling in CH_2Cl_2 solutions: (A) a 3 × 3 array; (B) the array in "A" after whittling at −385 mV vs Fc/Fc^+ for 60 s in 0.1 M $(CH_3CH_2)_4NBF_4$ methylene chloride solution; (C) a 3 × 3 array; (D) the same area in "C" after desorption at −460 mV vs Fc/Fc^+ for 60 s in 0.1 M $(CH_3CH_2)_4NBF_4$ methylene chloride solution. The bar is 500 nm.

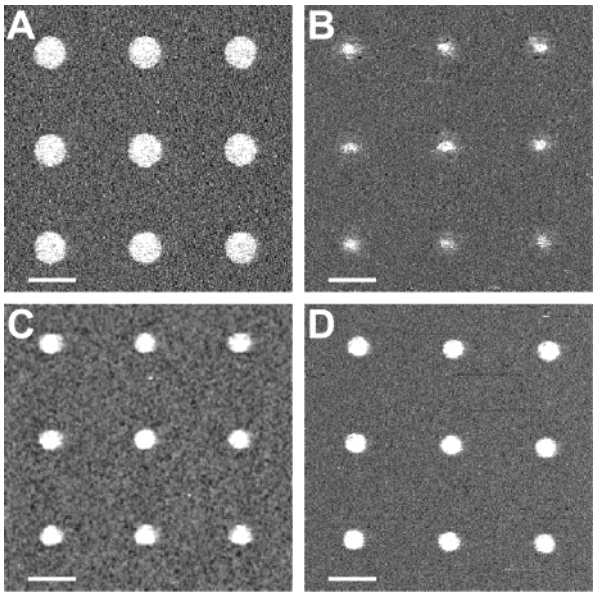

Figure 4. LFM images of MHA patterns: (A) 3 × 3 array; (B) the array in "A" after whittling at −1270 mV vs Fc/Fc^+ for 60 s in 0.1 M $[CH_3(CH_2)_3]_4NBF_4$ methylene chloride solution; (C) A 3 × 3 array; (D) the same array in "C" after whittling at −720 mV vs Fc/Fc^+ for 60 s in 0.1 M $[CH_3(CH_2)_3]_4NBF_4$ methylene chloride solution. The bar is 1 μm.

data, it is clear that the electrochemical whittling process is highly dependent upon the size of the charge compensating cation.

Finally, the electrochemical whittling of MHA nanostructures in organic media is not as controllable as it is in aqueous solutions, possibly because the MHA nanostructures are more disordered in organic solvents.[13] In general, inconsistent whittling rates were often observed in organic media and the resulting nanostructures were not as uniform as the ones obtained in aqueous media (compare Figure 4A,B with Figure 1). Note the standard deviations in whittling rates are significantly larger in organic media as compared with aqueous media (Table 1).

Effect of Surface Topography on the Electrochemical Whittling of MHA Nanostructures. The whittling rate and resulting feature uniformity are highly dependent upon the type of underlying gold substrate. In general, Au(111) substrates exhibit slightly slower whittling rates than polycrystalline substrates (Table 1). For example, at an electrode potential of −750 mV MHA features on Au(111) undergo the whittling process in aqueous media with KOH as the supporting electrolyte at a rate of 35 ± 9 nm/min, while on polycrystalline Au the rate is 50 ± 25 nm/min. Note that the standard deviation is only ∼25% of the average whittling rate, compared to ∼50% of that on polycrystalline Au surface. These results indicate that more ordered nanostructures with larger domain sizes, which form on single crystal terraces, undergo desorption almost exclusively from their perimeter sites.

In a typical experiment, ∼300 nm MHA dots (Figure 5A) formed on a Au(111) substrate were reduced to ∼230 nm structures by applying a potential of −750 mV for 2 min in 0.5 M aqueous KOH (Figure 5B). Moreover, after electrochemical whittling the peripheries of the MHA dots are very uniform. This is a consequence of uniform desorption from the edges of the features inward (compare Figure 5 with Figure 1). As with the polycrystalline gold the onset for whittling is at −750 mV, and no appreciable desorption is observed after holding the electrode at −700 mV for several minutes.

Electrochemical Whittling of Other Organic Nanostructures. The potential at which the electrochemical whittling process takes place is very dependent upon the type of headgroup. For example, features made from DODDSe begin to shrink at −450 mV, 400 mV less

(13) (a) Ravenscroft, M. S.; Finklea, H. O. *J. Phys. Chem.* **1994**, *98*, 3843. (b) Noh, J.; Hara, M. *Langmuir* **2001**, *17*, 7280.

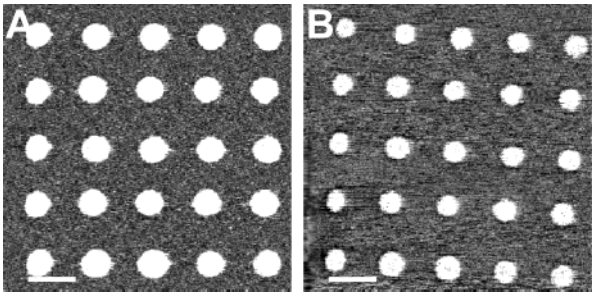

Figure 5. Electrochemical whittling of MHA nanostructures on Au(111) surface: (A) LFM image of an original MHA pattern on an Au(111) surface; (B) the same pattern in "A" after electrochemical whittling at −750 mV for 2 min in 0.5 M aqueous KOH solution. The bar is 500 nm.

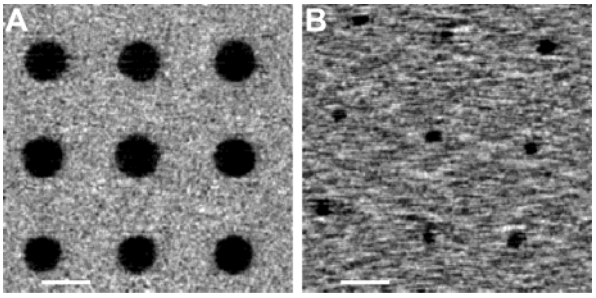

Figure 6. LFM images of a DPN-generated ODT pattern before (A) and after (B) electrochemical whittling at −1000 mV for 5 min in 0.5 M aqueous KOH solution. The bar is 1 μm.

negative than ODT (Table 1). Organoselenium SAMs have been prepared and characterized on gold by others.[14]

In 0.5 M aqueous KOH solution the reductive desorption peak in the cyclic voltammetry of a bulk SAM of ODT on a gold electrode is centered at around −1150 mV vs Ag/AgCl.[15] However, the onset of electrochemical whittling of ODT nanostructures was found to be −850 mV, and whittling could be effected at a reasonable rate at −1000 mV in 0.5 M KOH solution. For example, after holding a polycrystalline electrode, patterned with 900 nm dots of ODT, at −1000 mV for 5 min, the features were reduced to ~320 nm structures (Figure 6). In contrast, the reduction peak in the cyclic voltammetry of a bulk DODDSe SAM on a polycrystalline gold electrode in 0.5 M aqueous KOH solution is centered at −730 mV (Figure 7A). Our data indicate that the electrochemical whittling of DODDSe nanostructures generated by DPN can be controllably performed at −450 mV in 0.5 M KOH solution. DODDSe dot arrays before and after whittling at −450 mV for 2 min, respectively, exhibit a 150 nm reduction in dot diameter (Figure 7A,B).

Parallel Size Reduction of Organic Microstructures Fabricated by μCP. In principle, the electrochemical whittling method should be extendable to organic structures fabricated by processes other than DPN. Indeed, this is where the utility of the technique could be realized for miniaturizing microscale or relatively large nanoscale architectures in a massively parallel fashion. Many high-throughput printing, stamping, and photolithographic techniques that are challenged with respect to resolution could be used to make a set of larger features that could be subsequently miniaturized with the electrochemical whittling procedure. To test this hypothesis, we studied

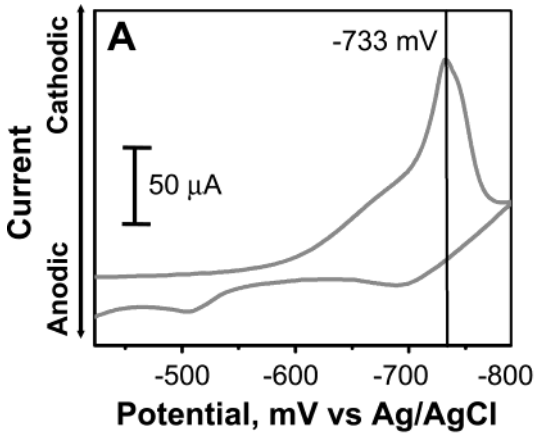

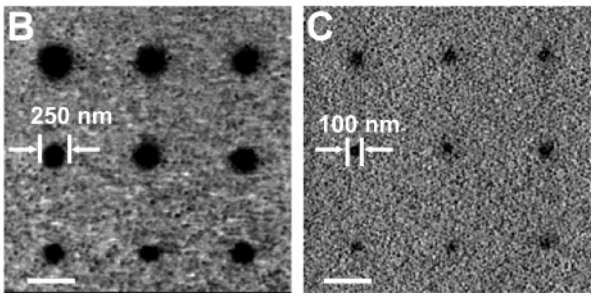

Figure 7. (A) Cyclic voltammogram for the reductive desorption of self-assembled monolayers of DODDSe on an Au substrate in 0.5 M aqueous KOH solution. The scan rate is 100 mV/s. (B, C) LFM images of a DPN-generated DODDSe pattern before (B) and after (C) electrochemical whittling at −450 mV for 2 min in 0.5 M aqueous KOH solution. The bar is 500 nm.

the method in the context of patterns of MHA and ODT made by μCP.

As proof-of-concept, 7 μm features made of MHA were generated on a polycrystalline gold substrate by the μCP method (Figure 8A). After a potential of −920 mV vs Ag/AgCl for 30 s in 0.5 M KOH aqueous solution was applied, each feature was reduced to $^1/_{10}$th of its original diameter. Some of the electrochemically whittled dots appear rough and are offset to some degree, which may be due to the local disorder of the original microstructures and subsequent nonuniform whittling. Similar experiments were carried out with 4 μm features of ODT generated by μCP (Figure 8C,D). After whittling at −1100 mV vs Ag/AgCl for 5 min in 0.5 M KOH aqueous solution, the ODT microstructures (Figure 8C) were reduced to ~3 μm structures (Figure 8D). The uniformity of the final structures is markedly dependent upon the magnitude of the reduction in size. In general, we find that one can shrink a structure by an order of magnitude (in diameter) without causing significant distortion under the optimized conditions reported herein.

The Role of Free Volume around Organic Nanostructures. The observations that the organic nanostructures can be electrochemically whittled from the perimeter inward and that the process is highly dependent on cation size indicate that the free volume around the organic nanostructures is essential to the whittling process. MHA molecules at the edge of nanostructures are less stable because there is greater accessibility of solvent molecules and ions to the electrode surface,[12a,16] which facilitates the whittling process. This hypothesis can be tested by filling the perimeter of the nanostructures

(14) (a) Samant, M. G.; Brown, C. A.; Gordon, J. G. *Langmuir* **1992**, *8*, 1615. (b) Dishner, M. H.; Hemminger, J. C.; Feher, F. J. *Langmuir* **1997**, *13*, 4788.

(15) Imabayashi, S.; Iida, M.; Hobara, D.; Feng, Z. Q.; Niki, K.; Kakiuchi, T. *J. Electroanal. Chem.* **1997**, *428*, 33.

(16) (a) Yang, D.-F.; Wilde, C. P.; Morin, M. *Langmuir* **1997**, *13*, 243. (b) Smith, C. P. and White, H. S. *Anal. Chem.* **1992**, *64*, 2398.

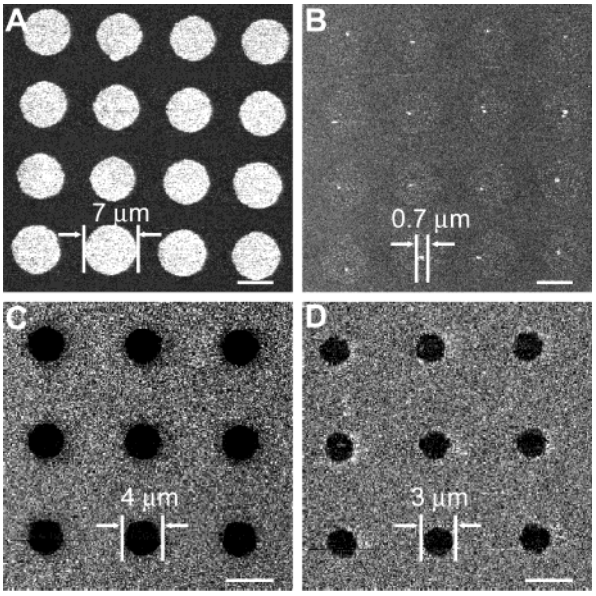

Figure 8. LFM images of μCP-generated patterns before and after electrochemical whittling. (A) Original MHA dots array. (B) The MHA dot array in the same area as in "A" after electrochemical whittling at a potential of −920 mV for 30 s in 0.5 M KOH solution. (C) Original ODT dot array. (D) The ODT dot array in the same area as in "C" after electrochemical whittling at a potential of −1100 mV for 5 min in 0.5 M KOH solution. The bar is 5 μm.

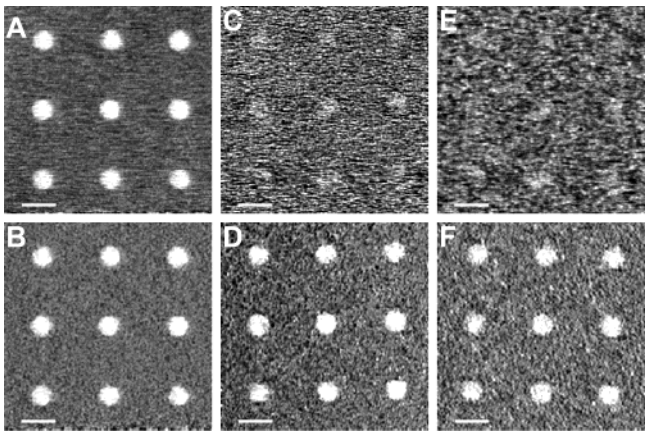

Figure 9. Topography (A, C, E) and LFM (B, D, F) images of a DPN-generated MHA dot array. (A, B) Original MHA array. (C, D) The same array in "A" and "B" after ODT passivation. (E, F) The same array in "C" and "D" after electrochemical desorption at −750 mV for 5 min in KOH solution. The bar is 500 nm.

with other molecules and examining the efficiency of the whittling process. Accordingly, ∼300 nm MHA nanostructures were generated on a gold substrate (Figure 9A,B, topographic and lateral force mode (LFM), respectively), and then the substrate was passivated with 5 mM ODT in ethanol solution for 1 min and washed with ethanol (Figure 9C,D). Finally, a −750 mV potential was applied to the substrate for 5 min in 0.5 M aqueous KOH solution (Figure 9E,F). LFM images indicate that very little desorption takes place under these conditions, and that which does, occurs in a nonuniform fashion (compare Figure 9B,D,F). In the topographic images, the DPN-generated MHA dots exhibited an average height of ∼2 nm before passivation (Figure 9A). After passivation with ODT, there is no appreciable height difference as one would expect. Significantly, this situation remains unchanged even after the attempted electrochemical whittling (Figure 9E), which shows that significant adsorbate desorption does not take place.

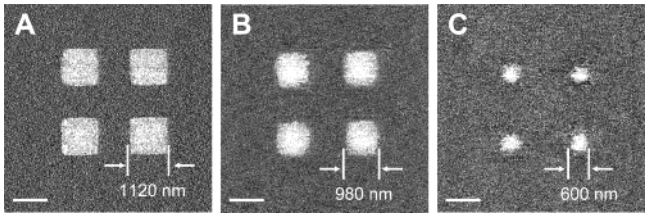

Figure 10. LFM images of DPN-generated MHA squares on a polycrystalline gold surface before and after electrochemical whittling: (A) original MHA squares; (B) the same MHA pattern as in "A" after electrochemical whittling in 0.5 M KOH solution at a potential of −750 mV for 3 min; (C) The same MHA pattern as in "B" after electrochemical whittling in 0.5 M KOH solution at a potential of −750 mV for another 7 min. The bar is 1 μm.

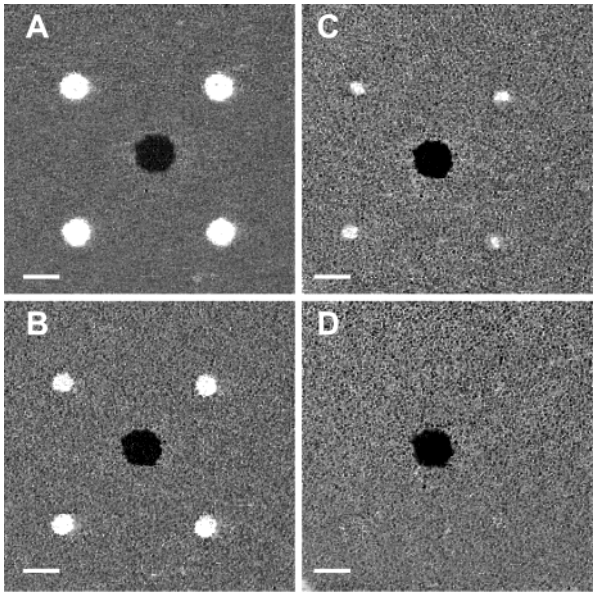

Figure 11. LFM images of ODT−MHA two-component array indicating selective whittling: (A) 2 × 2 array of MHA dots (white) and an ODT dot (black); the array in "A" after applying a potential of −750 mV for 3 min (B), 6 min (C), and 9 min (D), respectively. The bar is 500 nm.

The free volume near the MHA molecules at the vertexes of a nanostructure is larger, compared to the free volume near the straight edge sites. Therefore we hypothesized that the rate of whittling at vertexes sites would be faster than at the edge sites. Indeed, when electrochemical whittling was performed on DPN-generated MHA squares (Figure 10A), over extended periods of time desorption leads to structures with more circular shapes (Figure 10C). This limits how much one can miniaturize noncircular structures, without altering their shape.

Selective Whittling Based upon Different Tail Groups. By fine-tuning the electrochemical whittling conditions applied to a multicomponent array, in principle, various nanostructures can be addressed independently. To study this capability, we prepared a 2 × 2 MHA dot array with an ODT dot in the center (Figure 11A) on a gold surface and then applied a potential of −750 mV vs Ag/AgCl in 0.5 M aqueous KOH solution. Subsequent LFM images taken as a function of holding time (Figure 11B−D), show that the MHA dot features are gradually reduced in size while the ODT dot remains intact. This demonstrates that nanostructures can be independently addressed by making use of various desorption potentials, which in this case, can be attributed to a modification in the tail group. Nonetheless, further selectivity and tun-

ability can be achieved by altering a molecule's headgroup. For example, in contrast to the previous experiment, MHA dots remain intact while DODDSe are gradually whittled when a multi-ink array is exposed to a potential of −450 mV in 0.5 M KOH (Supporting Information).

Conclusion

In summary, we have systematically studied the desorption behavior of nano- and microscale SAM features on polycrystalline and atomically flat gold substrates. The desorption behavior is highly dependent upon cation size, electrolyte, substrate uniformity, SAM headgroup, SAM tail group, and applied potential. An understanding of this process allows one to controllably reduce feature size by selectively removing the adsorbates at the edge of a particular feature, moving inward. It is general with respect to alkanethiol inks and can be extended to printing methods such as μCP, provided the printing method generates features comprised of defect-minimized SAMs. Indeed, in our hands, we find that the quality of the array features generated from experiment to experiment are vastly different, and one needs to refine conditions to generate features that exhibit the uniform desorption properties reported herein.

This work is important for several reasons. First, it is a general method that is capable of increasing the resolution of resolution-limited high throughput lithographic or stamping processes. Indeed, this paper points toward a straightforward way of taking a set of microscopic structures and transforming them into nanometer scale structures in a massively parallel fashion. Second, new information regarding the electrochemical desorption of organic SAM-based structures has been revealed. Our results indicate that the free volume surrounding the organic structures plays an important role in electrochemical whittling. Finally, this study shows how one can tailor the addressability of different nanostructures within a multicomponent array through choice of SAM headgroup, SAM tail group, electrode potential, and electrolyte.

Acknowledgment. C.A.M. acknowledges the AFOSR, DARPA, and NSF for support of this research.

Supporting Information Available: LFM images of DPN-generated MHA patterns whittled in different electrochemical solutions and LFM images of selectivelty whittled DODDSe patterns. This material is available free of charge via the Internet at http://pubs.acs.org.

LA030392Y